

Short- and long-range correlations in the $S = \frac{1}{2}$ ferromagnetic chain system ($C_6D_{11}ND_3$)CuBr₃

K. Kopinga and W. J. M. de Jonge

Department of Physics, Eindhoven University of Technology, P.O. Box 513, NL-5600 MB Eindhoven, The Netherlands

M. Steiner

Hahn-Meitner Institut für Kernforschung G.m.b.H., Glienickerstrasse 100, D-1000 Berlin 39, Federal Republic of Germany

G. C. de Vries and E. Frikkee

Netherlands Energy Research Foundation ECN, P.O. Box 1, NL-1755 ZG Petten, The Netherlands

(Received 21 January 1986)

The short- and long-range spin correlations in the quasi-one-dimensional $S = \frac{1}{2}$ system ($C_6D_{11}ND_3$)CuBr₃ (CHAB-D14) have been investigated by (quasi) elastic neutron scattering experiments. The temperature dependence of the sublattice magnetization below $T_N = 1.56$ K reflects the presence of ferromagnetic chains in this compound. The intrachain spin correlations in the paramagnetic region show a crossover from isotropic Heisenberg behavior at high temperatures to XY behavior below ~ 3 K, and are surprisingly well described by a classical spin model.

I. INTRODUCTION

The fact that the one-dimensional (1D) $S = \frac{1}{2}$ spin system with a ferromagnetic nearest-neighbor interaction is a very simple model system in the extreme quantum limit has stimulated extensive theoretical studies on this class of systems.^{1,2} Despite these activities, exact results for the static and dynamic properties are at present only available for a few special cases. On the other hand, experimental studies on these systems are still rather scarce.

One of the best realizations of a 1D $S = \frac{1}{2}$ ferromagnetic system known at this moment is ($C_6H_{11}NH_3$)CuBr₃ (CHAB). The intrachain interaction in this compound exceeds the coupling between the chains by three orders of magnitude.³ Its static properties have been established by heat-capacity and magnetization measurements and may be described by an intrachain interaction $J/k_B = 55 \pm 5$ K containing about 5% XY anisotropy. The $q=0$ part of the dynamic form factors $\mathcal{S}^{\alpha\alpha}(\mathbf{q}, \omega)$ (Ref. 2) has been investigated by ferromagnetic-resonance (FMR) experiments.⁴ The field dependence of the signals observed at low temperatures could be interpreted in terms of standard spin-wave theory. The analysis confirmed the general characteristics mentioned above and revealed, in addition, that the anisotropy within the XY plane is very small; $(J^{xx} - J^{yy})/J^{xx} \approx 5 \times 10^{-4}$, i.e., 1% of the XY anisotropy itself. Additional information on the elementary excitations in CHAB was obtained from measurements of the nuclear spin-lattice relaxation time and the field dependence of the heat capacity $\Delta C(B) = C(B) - C(B=0)$.⁵ It appeared that spin-wave theory failed to describe even the qualitative behavior of $\Delta C(B)$, suggesting that nonlinear processes in this compound may be very important, at least in a certain range of field and temperature. In view of the easy-plane anisotropy in J , the observed behavior was interpreted in terms of the sine-Gordon model, which was found to yield a fair

description of the data. A more detailed analysis of the heat capacity, however, revealed that the applicability of this classical model to the $S = \frac{1}{2}$ system CHAB resulted from an accidental canceling of the quantum sine-Gordon corrections by the effect of spin components out of the easy plane.^{6,7}

In view of the results summarized above and the still rather incomplete theoretical description of the present class of model systems we have started a detailed study of the static and dynamic magnetic properties of CHAB by means of neutron scattering experiments. In this paper we shall report on the first part of this study, dealing with the three-dimensional (3D) long-range order and the quasistatic 1D spin correlations in the fully deuterated compound ($C_6D_{11}ND_3$)CuBr₃ (CHAB-D14). The organization of the paper is as follows. In Sec. II we shall briefly review the crystallographic and magnetic properties of hydrogenated and deuterated CHAB. The behavior of the 3D-order parameter in CHAB-D14 will be discussed in Sec. III, whereas Sec. IV will be devoted to the temperature dependence of the intrachain spin correlations. The paper will be concluded with a discussion in Sec. V.

II. CRYSTALLOGRAPHIC AND MAGNETIC PROPERTIES

In contrast to the chlorine compound ($C_6H_{11}NH_3$)CuCl₃ (CHAC, Ref. 8), the crystallographic structure of CHAB has not yet been reported in detail. Powder x-ray diffraction measurements on both hydrogenated and deuterated CHAB indicate that also the bromine compounds have an orthorhombic structure, with $a = 19.84$ Å, $b = 8.78$ Å, and $c = 6.44$ Å (300 K), space group $P2_12_12_1$, and four formula units in the crystallographic unit cell. This is supported by single-crystal neutron diffraction experiments on CHAB-D14. The powder

measurements reveal that the fractional coordinates of the heavy atoms within the unit cell of this compound are only slightly different from those in CHAB-H14 and CHAC. A detailed report on the synthesis and structure of CHAB-D14 will be published elsewhere.⁹

Preliminary FMR and magnetization measurements on CHAB-D14 yield results that are identical to those on CHAB (Refs. 3 and 4) within experimental inaccuracy, which suggests that deuteration of this compound has only a small effect on the magnetic properties. The magnetic array consists of $-\text{Cu}-\text{Br}_3-\text{Cu}-\text{Br}_3-$ chains running along the crystallographic c direction. The magnetic properties of the individual chains can be described by the Hamiltonian

$$H = -2 \sum_i (J^{xx} S_i^x S_{i+1}^x + J^{yy} S_i^y S_{i+1}^y + J^{zz} S_i^z S_{i+1}^z), \quad (1)$$

with $J^{xx}/k_B = 55 \pm 5$ K, $J^{zz}/J^{xx} = 0.95$, and $(J^{xx} - J^{yy})/J^{xx} \approx 5 \times 10^{-4}$. The y axis coincides with the crystallographic c axis, whereas the x axis is located within the ab plane at an angle φ from the b axis. Two symmetry-related types of chains are present, with $\varphi = -25^\circ$ and $+25^\circ$, respectively. We wish to stress that the XY character of the intrachain interaction in CHAB originates from the symmetry of the local environment of the Cu^{2+} ions, which explains the fact that the easy XY planes are not perpendicular to the chain direction, like in tetramethylammonium manganese trichloride (TMMC) and CsNiF_3 .¹⁰

The weak coupling between the chains induces a 3D noncompensated antiferromagnetic ordering below $T_N = 1.50$ K for CHAB-H14.³ If we assume that the magnetic space group of this compound belongs to the Opechowski family¹¹ of the space group $P2_12_12_1$, only the magnetic space group $P2_12_1'2_1'$ satisfies the requirements imposed by the experimental observations, viz., the presence of ferromagnetic chains along c , magnetic moments located within the ab plane, and a net ferromagnetic moment along the a direction. Although this magnetic space group in principle allows a canting of adjacent moments within each chain towards the positive and negative c direction, respectively, FMR rotation diagrams demonstrate that such a canting—if actually present—amounts to less than 2° . We like to note that the spin structure below T_N is similar to that inferred for CHAC (Ref. 8) from arguments relating the strength and sign of the various interactions in this compound to the possible superexchange paths.

III. LONG-RANGE ORDER

In order to investigate the development of long-range order below T_N in CHAB-D14, neutron-diffraction experiments were performed on the D1S spectrometer at the reactor BER II in two-axis configuration. A wavelength of 1.715 Å was used, obtained from the Ge(311) reflection. A 30' Soller slit collimator was placed in front of the detector. The vertical collimation and the horizontal divergence of the incoming neutron beam ($\sim 1^\circ$) were determined by the geometry of the diffractometer. A single crystal of CHAB-D14 with dimensions $a \times b \times c = 5 \times 2 \times 18$ mm³ was mounted in a ³He cryostat

with the c axis vertical. Sample temperatures between 0.39 and 2 K could be maintained with a typical stability of a few mK.

For the 3D magnetic structure, conjectured in Sec. II, the strongest magnetic Bragg reflection in the a^*b^* scattering plane is expected at (100). Because, moreover, in an ideal $P2_12_12_1$ structure the ($h00$) nuclear Bragg reflections with odd h are systematically absent, the (100) position was selected to monitor the temperature dependence of the 3D antiferromagnetic order of the components μ_b . Below $T \approx 1.6$ K, a significant increase of intensity was observed, which at the lowest attainable temperature (0.39 K) did amount to $\approx 6\%$ of the intensity of the strongest nuclear reflection (310) in the a^*b^* plane.

Figure 1 shows the resulting temperature dependence of the sublattice magnetization M_s , which in CHAB is proportional to $\langle \mu_b \rangle$, since the direction of the moments within the ab plane is fixed by the easy-hard anisotropy.⁴ The data, corresponding to the square root of the intensity after subtraction of the background observed at $T = 2$ K, are represented by open circles. From extrapolation of a smooth curve through the data the ordering temperature is found as $T_N = 1.56 \pm 0.02$ K. This result is rather close to the value $T_N = 1.50$ K for CHAB-H14, which confirms that deuteration of CHAB has only a small effect on the magnetic properties.

The low-temperature behavior of the sublattice magnetization seems somewhat unusual, in the sense that it continues to increase down to very low temperatures. This behavior, which in fact indicates the presence of a large density of states at low energy in this compound, can be understood—at least qualitatively—within the framework of conventional mean-field (MF) theory. In Fig. 1 we included the MF predictions for $S = \frac{1}{2}$ and for a classical ($S = \infty$) system. Inspection of this figure shows that the qualitative behavior of the data resembles that of the classical MF model rather than that of the $S = \frac{1}{2}$ model. This may result from the presence of ferromagnetic chains in this compound, which behave as “rigid” entities

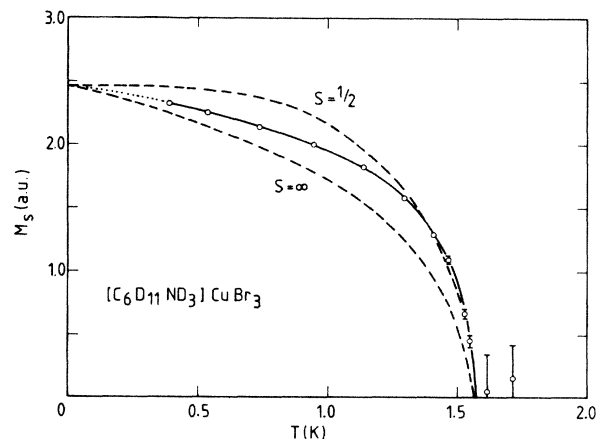


FIG. 1. Temperature dependence of the order parameter M_s in CHAB-D14 deduced from the magnetic Bragg intensity at (100). The data are represented by open circles, whereas the solid curve is meant as a guide to the eye. Error bars are plotted only if they exceed the size of the data points. Broken curves reflect mean-field predictions.

with a large value of S if $k_B T/J \ll 1$. These entities are weakly coupled in a two-dimensional array by the inter-chain interactions. If this simplified picture holds, the quantitative deviations between the classical MF model and the data at low T might be attributed to dimensionality effects, since in general a reduction of dimensionality causes the sublattice magnetization in this region to vary more slowly with T than that of the corresponding MF prediction. Such a conclusion, however, should be considered with some reservations, because the presence of anisotropy is known¹² to have a similar effect.

IV. 1D SHORT-RANGE ORDER

The development of magnetic correlations within the individual chains in CHAB-D14 in the paramagnetic region was investigated by quasielastic neutron scattering experiments. For this purpose a single crystal with dimension $5 \times 14 \times 23 \text{ mm}^3$ was mounted in a ^4He cryostat with both the c^* and the $[110]$ directions within the scattering plane. Part of the experiments were performed on the DIS spectrometer at BER II in two-axis configuration using a wavelength of 1.715 Å. The data were supplemented with measurements at the High Flux Reactor (HFR) in Petten. In the latter case a wavelength of 1.497 Å was used, obtained from a Zn(002) monochromator. Sample temperatures between 1.5 and 10 K could be maintained with a long-time stability of about 20 mK. At the highest experimental temperature ($\approx 55 \text{ K}$), the stability was about 0.5 K.

The presence of ferromagnetic intrachain correlations in this compound will give rise to diffuse scattering with maximum intensity in planes in reciprocal space perpendicular to c^* at $l=2n$, because the spin-spin distance equals $c/2$. The scattering cross section along a direction normal to such a plane, resulting from correlations between the α components of the spins, can be approximated by a Lorentzian, which can be written as^{10,13}

$$(d\sigma/d\Omega)_\alpha = A_\alpha \mathcal{L}^{\alpha\alpha}(q) = A_\alpha \kappa_\alpha^2 \chi^{\alpha\alpha}(0) / (\kappa_\alpha^2 + q^2). \quad (2)$$

In this equation A_α is a proportionality constant, $\alpha=x,y,z$, κ_α is the so-called inverse correlation length for the spin components S^α , $\chi^{\alpha\alpha}(0)$ is the magnetic susceptibility of the chain along α , and q is the distance to the plane.

In the present experiments, the optimum configuration for quasielastic measurements, i.e., the wave vector of the scattered neutrons parallel to the plane,¹⁴ would be realized for suitably chosen scans through the $l=2$ plane. Unfortunately, such scans did not reveal any significant change of the scattered intensity between 2 and 55 K, due to the reduction of intensity by the magnetic form factor and the unfavorable orientation of the resolution contour with respect to the plane. For this reason, scans were performed normal to the $l=0$ plane, in which the scattered intensity was enhanced by increasing the horizontal and vertical divergence to the limit set by the geometry of the diffractometer ($\approx 1^\circ$). The resulting resolution contour in the scattering plane, determined experimentally at the (110) Bragg reflection, is depicted in the inset of Fig. 2. In this configuration, the intensity observed in the $l=0$

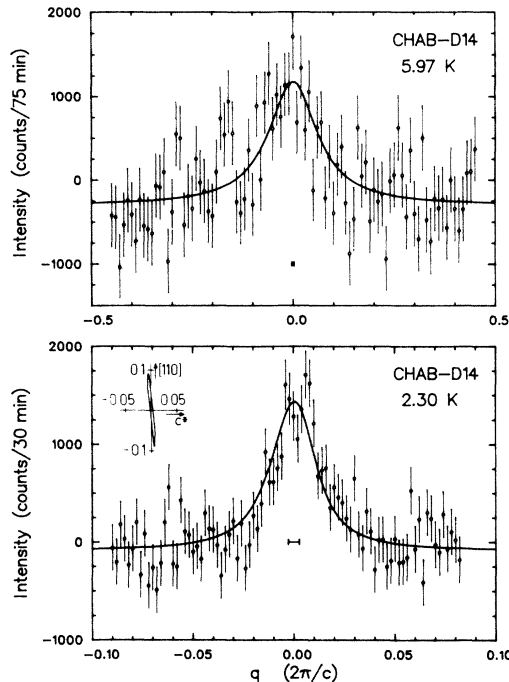


FIG. 2. Neutron scattering intensities observed at 2.30 and 5.97 K along $(0.78, 0.78, \xi)$ corrected for the intensity at 55 K. The solid curves are best fits to the data of the convolution of a Lorentzian with the experimental resolution. Note the difference in scale for the two scans. The resolution contour around $(0.78, 0.78, 0)$ is plotted in the inset, whereas the effective width of the resolution along c^* is depicted at the center of the scans.

plane was found to increase by a few percent when the temperature was lowered from 55 to 2 K. The intensity profile perpendicular to the plane between 1.5 and 10 K was studied by scans along $\mathbf{Q}=(0.36, 0.36, \xi)$ and $(0.78, 0.78, \xi)$ at BER II and the HFR in Petten, respectively. After subtraction of the intensity, observed in similar scans at 55 K, the data were analyzed by least-squares fits of the convolution of a Lorentzian [cf. Eq. (2)] with the experimental resolution function $R(q)$. Since the magnetic scattering occurs in planes perpendicular to the scattering plane, the resolution in the vertical direction has no effect on the deconvolution procedure. In the analysis we had to include a q -independent term in order to account for the small differences in the background intensity during subsequent reactor cycles.

As an example, the data collected at 2.30 and 5.97 K, corrected for the background, are plotted in Fig. 2. The solid curves represent the results of the analysis outlined above. The resulting inverse correlation lengths are plotted in Fig. 3 as κ/T against T . Included in the figure are several theoretical predictions, all of which are calculated without any adjustable parameters, i.e., using the exchange and anisotropy parameters, which are appropriate to CHAB (cf. Sec. II). The dashed curve represents the temperature dependence of the inverse correlation length of a fully isotropic Heisenberg system of classical spins, given by¹⁰

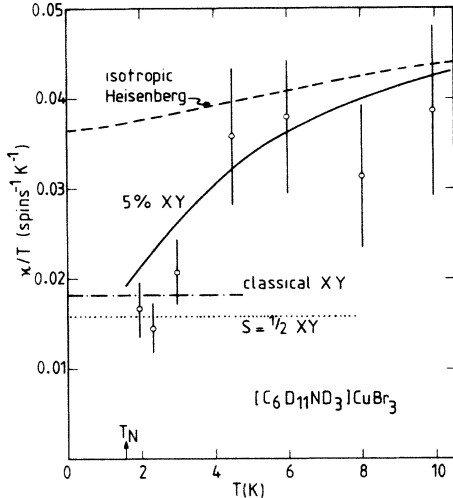


FIG. 3. Temperature dependence of the inverse correlation length κ along the chains of CHAB-D14, plotted as κ/T against T . Experimental data are represented by open circles. The various theoretical predictions are discussed in the text.

$$\kappa = -\ln \left[\coth \left| \frac{2JS^2}{k_B T} \right| - \frac{k_B T}{2JS^2} \right], \quad (3)$$

for $J/k_B = J^{xx}/k_B = 55$ K. It should be emphasized that in all calculations we use classical spins with a “length” equal to the spin quantum number S rather than the value $\sqrt{S(S+1)}$ resulting from a semiclassical approximation. We will return to this point in the Discussion. Above $T \approx 4$ K, Eq. (3) describes the observed correlation length fairly well. In fact, if we would have used a value $J/k_B = 60$ K, which is within the uncertainty limits given in Sec. II, a very good agreement between theory and experiment would have been obtained in this temperature region. At lower temperatures, however, the experimental results for κ drop significantly below the prediction for the isotropic case. The data seem to approach the inverse correlation length for the classical XY model, given by $\kappa = k_B T / 4JS^2$ at low T . This prediction for $J/k_B = 55$ K is represented by the dashed-dotted line in Fig. 3. The apparent crossover from Heisenberg behavior at high temperatures to XY behavior below $T \approx 3$ K is correctly described by transfer-matrix calculations¹⁵ of the correlation length of the spin components within the easy plane for a chain of classical spins using the full set of exchange and anisotropy parameters given in Sec. II. The results of these calculations are represented by the solid curve in the figure.

Because CHAB is an $S = \frac{1}{2}$ system, it would be preferable to compare the experimental data with calculations of the correlation length in a real quantum model system. To our knowledge, however, theoretical results are only available for the $S = \frac{1}{2}$ XY system,¹⁶ which we have represented by the dotted line in Fig. 3, corresponding to $J/k_B = 55$ K. The relation of this prediction to the other results presented in this figure will be discussed in the following section.

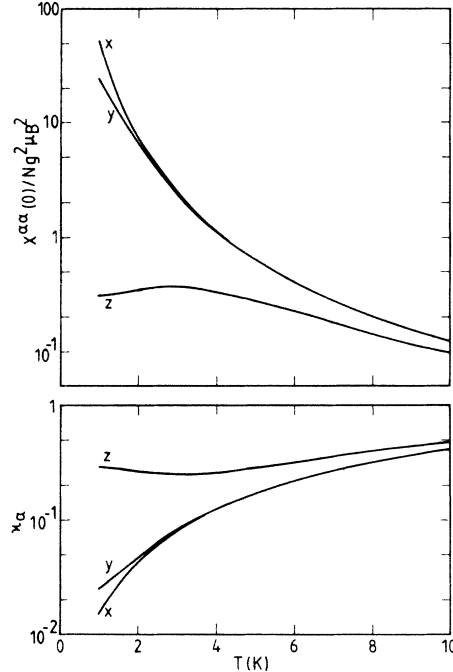


FIG. 4. Predicted temperature dependence of the magnetic susceptibility $\chi^{\alpha\alpha}(0)$ and the inverse correlation length κ_α along the chains in CHAB for the spin components along the easy (x), intermediate (y), and hard (z) directions. The results are obtained from transfer-matrix calculations on a one-dimensional classical spin model with $J^{xx}/k_B = 55$ K, $J^z/J^{xx} = 0.95$, and $(1 - J^{yy}/J^{xx}) = 5 \times 10^{-4}$. κ is expressed in units of the inverse spin distance.

V. DISCUSSION

From the comparison of the experimental data with theoretical predictions in Sec. IV it is obvious that transfer-matrix calculations of the inverse correlation length of a chain of classical spins, based on the spin Hamiltonian and interaction parameters inferred from heat-capacity and FMR experiments^{3,4} yield a surprisingly good description of the actual data on κ for the present $S = \frac{1}{2}$ system. As already mentioned above, we have used a classical interaction energy $2JS^2$ instead of the semiclassical value $2JS(S+1)$.¹⁰ In the latter case, the theoretical prediction for κ/T presented in Fig. 3 would have been shifted downwards by about a factor of 3, which would be far below the experimental data. This tendency is consistent with the interpretation of the excess heat capacity of CHAB-H14 in terms of the classical sine-Gordon model,⁶ which also indicated that the spin length can be chosen equal to the spin quantum number S . To some extent, this choice is supported by the rather good quantitative agreement between the behavior of κ calculated for the classical XY and for the $S = \frac{1}{2}$ XY model, as can be seen in Fig. 3.

A few aspects of the present interpretation should be emphasized. In the evaluation of κ , we tacitly assumed a Lorentzian intensity profile [cf. Eq. (2)], which corresponds to an exponential decrease of the spin-spin correla-

tions $\langle S_i^\alpha S_{i+m}^\alpha \rangle$ with distance m , as in the isotropic classical spin model. For the anisotropic classical spin model¹⁷ and the $S = \frac{1}{2}$ XY model,¹⁶ such an exponential decrease occurs only for large values of m . Unfortunately, the very weak magnetic scattering in our experiments precludes a detailed analysis of the line shape. Therefore, we tried to estimate the implication of this approximation by comparing the full width at half maximum (FWHM) of the reported wave-number-dependent spin pair-correlation function $\mathcal{S}(q)$ of the $S = \frac{1}{2}$ XY model with that of a Lorentzian curve corresponding to the same value of κ . This comparison revealed that the width of the Lorentzian exceeds that of $\mathcal{S}(q)$ by about 20% at the lowest temperatures. For the classical spin model with anisotropy parameters appropriate to CHAB, the deviations are found to be smaller by almost one order of magnitude, and hence do not affect the interpretation given in Sec. IV.

Finally, we comment on the crossover region. In the experiments reported in Sec. IV the diffuse intensity has been recorded transverse to the [110] direction in reciprocal space. At the center of the scan the scattering vector \mathbf{Q} is located in the ab plane at an angle of 23.8° from b . Since only spin components perpendicular to \mathbf{Q} contribute to the scattering, it can be deduced from the magnetic structure of CHAB, presented in Sec. II, that the proportionality constants A_α in Eq. (2) have a relative magnitude of 0.28, 1.0, and 0.72 for the spin components along the easy (x), intermediate (y), and hard (z) directions, respectively. Apart from this, the contribution of these spin components to the intensity near $q=0$ is proportional to the corresponding susceptibilities $\chi^{\alpha\alpha}(0)$; $\alpha=x,y,z$. The implications for our experiments are illustrated in Fig. 4, where we present results of transfer-matrix calculations of κ_α and $\chi^{\alpha\alpha}(0)$, obtained for the set of parameters

appropriate to CHAB. From this figure it is obvious that the correlations between the spin components along the hard axis are markedly different from those between the components along the easy and intermediate axes. In principle, this behavior complicates the interpretation of the present data. At $T \geq 8$ K, however, the difference between κ_x and κ_z decreases to about 10%, and hence the systematic error caused by fitting the scattering profile by a single Lorentzian is of the same order of magnitude as the experimental uncertainty. For $T \leq 3$ K, on the other hand, the susceptibility along the hard axis, $\chi^z(0)$, is more than a factor of 10 smaller than $\chi^{xx}(0)$ and $\chi^{yy}(0)$, and therefore the intensity is almost completely determined by the spin components within the easy plane. Therefore, we conclude that outside the cross-over region ($3 \text{ K} < T < 8 \text{ K}$) the analysis of the scattering profile is—in principle—straightforward. Unfortunately, the magnetic scattering above 10 K was too weak to enable a quantitative analysis of the data. On the other hand, the intensity profile below 2 K has not been analyzed in detail, since at these temperatures the observed magnetic scattering decreased significantly. This is most likely due to the development of 3D spin correlations, which cause the intensity to contract towards magnetic Bragg peaks.

ACKNOWLEDGMENTS

We would like to thank Professor E. F. Godefroi (Department of Chemistry, Eindhoven) for the synthesis of deuterated cyclohexylamine. We are much indebted to A. M. C. Tinus for his help in the transfer-matrix calculations and to W. A. H. M. Vlak for his help in the data analysis. Two of the authors (K.K. and G.d.V.) wish to thank the group C1 of the Hahn-Meitner Institut for their hospitality during their stay.

¹See, for instance, J. D. Johnson and J. C. Bonner, *Phys. Rev. B* **22**, 251 (1980), and references therein.

²T. Schneider and E. Stoll, *Phys. Rev. B* **25**, 4721 (1982); T. Schneider, E. Stoll, and U. Glaus, *Phys. Rev. B* **26**, 1321 (1982).

³K. Kopinga, A. M. C. Tinus, and W. J. M. de Jonge, *Phys. Rev. B* **25**, 4685 (1982).

⁴A. C. Phaff, C. H. W. Swüste, W. J. M. de Jonge, R. Hoogerbeets, and A. J. van Duyneveldt, *J. Phys. C* **17**, 2583 (1984).

⁵K. Kopinga, A. M. C. Tinus, and W. J. M. de Jonge, *Phys. Rev. B* **29**, 2868 (1984).

⁶A. M. C. Tinus, W. J. M. de Jonge, and K. Kopinga, *Phys. Rev. B* **32**, 3154 (1985).

⁷M. D. Johnson and N. F. Wright, *Phys. Rev. B* **32**, 5798 (1985).

⁸H. A. Groenendijk, H. W. J. Blöte, A. J. van Duyneveldt, R. M. Gaura, C. P. Landee, and R. D. Willett, *Physica* **106B**, 47 (1981).

⁹G. C. de Vries *et al.* (unpublished).

¹⁰M. Steiner, J. Villain, and C. G. Windsor, *Adv. Phys.* **25**, 87 (1976).

¹¹W. Opechowski and R. Gucione, in *Magnetism*, edited by G. Suhl and H. Rado (Academic, New York, 1965), Vol. 2A, Chap. 3.

¹²These general tendencies are observed in many systems; an extensive review can be found in L. J. de Jongh and A. R. Miedema, *Adv. Phys.* **23**, 1 (1974).

¹³J. M. Loveluck, S. W. Lovesey, and S. Aubry, *J. Phys. C* **8**, 3841 (1975).

¹⁴R. J. Birgeneau, J. Skalyo, Jr., and G. Shirane, *Phys. Rev. B* **3**, 1736 (1971).

¹⁵F. Boersma, K. Kopinga, and W. J. M. de Jonge, *Phys. Rev. B* **23**, 186 (1981).

¹⁶T. Tonegawa, *Solid State Commun.* **40**, 983 (1981).

¹⁷M. Blume, P. Heller, and N. A. Lurie, *Phys. Rev. B* **11**, 4483 (1975).